Gamma-ray irradiation effect on deuterium retention in reduced activation ferritic/martensitic steel and ceramic coatings

Shota Nakazawa[a], Kazuki Nakamura[a], Hikari Fujita[b], Hans Maier[c], Thomas Schwarz-Selinger[c], Yuji Hatano[d], Naoko Ashikawa[e,f], Wataru Inami[a], Yoshimasa Kawata[a], Takumi Chikada[a*]

[a]Shizuoka University, Shizuoka, Japan

[b]The University of Tokyo, Tokyo, Japan

[c]Max-Planck-Institut für Plasmaphysik, 85748 Garching, Germany

[d]University of Toyama, Toyama, Japan

[e]National Institute for Fusion Science, Gifu, Japan

[f]The Graduate University for Advanced Studies, Gifu, Japan

*Corresponding author's email: chikada.takumi@shizuoka.ac.jp

Abstract

Tritium permeation and retention are serious problems in D-T fusion reactors from the viewpoint of fuel efficiency and radiological safety. Functional ceramic coatings have been intensively studied for the development of tritium permeation barrier for several decades, while reports about tritium retention in the ceramic coatings are absolutely scarce. Moreover, irradiation may effect on tritium retention in fusion materials, which is important to precisely evaluate tritium inventory in the reactor. In this study, the gamma-ray irradiation effect on deuterium retention in reduced activation ferritic/martensitic steel and three ceramic coatings were investigated through deuterium exposure,

gamma-ray irradiation using cobalt-60 gamma-ray sources and deuterium depth profile measurements. The amount of deuterium retention in yttrium oxide, silicon carbide and zirconium oxide coatings decreased after the irradiation in the dose rate of 2.43 Gy/s, while no clear change in the retention was observed at the lower dose rate. From these results, the gamma-irradiation effect on deuterium retention would have a threshold dose rate. Diffusion and desorption of deuterium would be accelerated by excitation of deuterium via energy transfer from electrons generated by Compton scattering.

Keywords: Hydrogen isotope, Retention, Gamma-ray irradiation, Reduced activation ferritic/martensitic, Ceramics coating

1. Introduction

One of critical challenges for the realization of a D-T fusion reactor is tritium permeation through structural materials, which causes a reduction of fuel efficiency and environment pollution. In order to suppress the permeation, tritium permeation barrier (TPB) coatings have been developed for several decades. Oxide, nitride and carbide coatings fabricated by various methods showed high deuterium permeation reduction performance in the previous studies [1–4]. Another critical problem is tritium inventory, which drastically varies fuel efficiency as permeation. Hydrogen isotope inventory in the TPB coatings has also been investigated in our previous studies [5,6]. These papers revealed that the amount of deuterium retention in ceramic coatings was much larger than that in steels. However, the blanket materials including TPB coatings are exposed to high dose neutrons and gamma-rays in an actual reactor, which may vary tritium retention even more drastically. In our previous studies, deuterium permeation behaviors through metals and the coatings under gamma-ray irradiation have been investigated [7,8], and an increase of deuterium permeation flux was confirmed during gamma-ray irradiation. Therefore, gamma-ray irradiation may also affect the hydrogen isotope retention behavior in the blanket materials. Moreover, it is important to discriminate the effect of gamma-ray from that of neutron for elucidation of pure gamma-ray irradiation effects, leading to understanding of multiple irradiation effects on hydrogen isotope migration behavior in the fusion reactor. On the other hand, few reports about gamma-ray irradiation effects on hydrogen isotope retention behavior in fusion materials are available.

In this study, reduced activation ferritic/martensitic (RAFM) steel F82H and representative three kinds of ceramic coatings: yttrium oxide (Y_2O_3), silicon carbide (SiC) and zirconium oxide (ZrO_2) coatings were chosen as candidates of the structural materials and TPB, and gamma-ray irradiation effects on deuterium retention behavior in the samples were investigated through deuterium depth profiling after deuterium exposure and gamma-ray irradiation experiments.

2. Experimental details

2.1. Sample preparation and analysis

RAFM steel F82H (Fe-8Cr-2W, F82H-BA07 heat) plates with dimensions of 25-mm length, 25-mm width and 0.5-mm thickness were used as samples and substrates for Y_2O_3, SiC and ZrO_2 coatings. Y_2O_3 and SiC coatings were prepared by non-reactive radio-frequency magnetron sputtering (MS, Sanyu Electron Co., Ltd., SVC-700RF). After evacuation of a chamber (~10^{-3} Pa), argon gas was introduced to generate a plasma with 10 sccm (standard cubic centimeter per minute). During the deposition, the argon pressure was kept to 1 Pa, and the input power was 50 W. The sample temperature rose up to about 100 ºC during deposition. The Y_2O_3-coated samples were heat-treated for 24 h at 600 ºC under high vacuum (10^{-6}–10^{-5} Pa) to promote crystallization as conducted in our previous study [2]. The heat treatment was not performed for the SiC coatings because the coating had a non-crystalline structure and showed no significant change in microstructure after annealing [3]. ZrO_2 coatings were fabricated by metal organic decomposition (MOD) after the formation of a

chromium oxide (Cr_2O_3) layer that improves adhesion between the coating and the substrate [9]. The MOD procedure followed the previous paper [10]. The Cr_2O_3-formed substrates were dipped into a ZrO_2 precursor (Kojundo Chemical Laboratory Co., Ltd., SYM-ZR04®, Zr concentration: 0.4 mol/L) and withdrawn at a constant speed of 1.0 mm s^{-1}, followed by drying at 150 ºC for 6 min and pre-heating at 550 ºC for 2 min in air using hot plates. This process was repeated for 6 times to increase the coating thickness. After that, the samples were heat-treated at 700 ºC for 30 min under Ar and H_2 mixture flow (Ar:H_2 = 1:1). A series of the process including the heat treatment was repeated twice.

Crystal structure and grain size of the coatings were examined by grazing incidence X-ray diffraction (GIXRD, RINT 2200, Rigaku Co. Ltd.) using an X-ray source of Cu Kα (1.5418 Å) with Scherrer's equation. Chemical composition and bonding state were analyzed by X-ray photoelectron spectroscopy (XPS, PHI 5000 VersaProbe, ULVAC-PHI, Inc.) with an X-ray source of Al Kα (1486.6 eV). The sample surfaces were sputtered for depth analysis using a 2 kV Ar ion gun with the sputtering rate of approximately 10 nm min^{-1}.

2.2. Deuterium exposure experiment

The uncoated and coated samples were cut into about 10-mm squares. Deuterium exposure was performed using a vacuum apparatus shown in Fig. 1. The samples were put into a metal chamber connecting a vacuum system and heated up to 500 ºC by an electric furnace under the pressure range of 10^{-5}–10^{-3} Pa. After the temperature reached 500 ºC, deuterium gas at 80 kPa was introduced into

the chamber and maintained for 50 h. Then the chamber was air-cooled to room temperature with the samples exposed to deuterium. Each sample was immediately encapsulated into a vial container under argon atmosphere in a glove box.

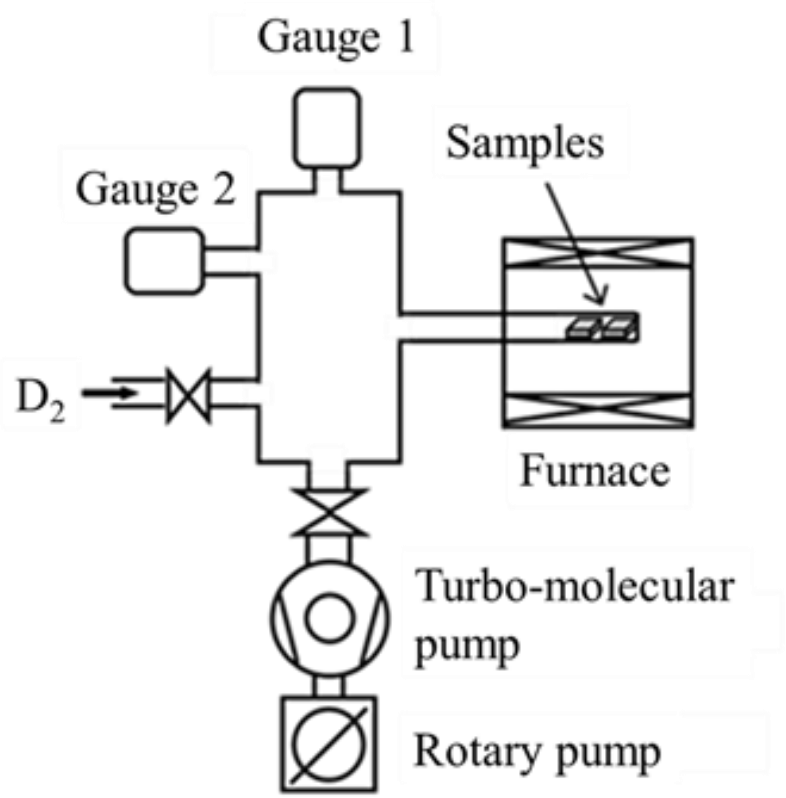

Fig. 1 Conceptional scheme of deuterium exposure apparatus.

2.3. Gamma-ray irradiation experiment

Gamma-ray irradiation experiments were conducted with cobalt-60 (^{60}Co) sources at Shizuoka University and Takasaki Advanced Radiation Research Institute, National Institutes for Quantum and Radiological Science and Technology (QST). Table 1 shows irradiation parameters for the uncoated and coated samples. In the experiments at Shizuoka University, the dose rates were calculated to be

approximately 0.084–0.384 Gy s^{-1}, and the samples were irradiated with the doses of 1, 10 and 100 kGy in iron equivalent. In the experiments at QST, the dose rate was estimated to be 2.43 Gy s^{-1}, and the samples were irradiated with the dose of up to 1280 kGy. All the irradiation experiments were conducted at room temperature. The increase of sample temperature during irradiation, which is called gamma heating, was less than 10 ºC in this work; therefore, the temperature effect on deuterium retention in the materials would be small.

2.4. Deuterium depth profiles by nuclear reaction analysis

Depth profiles of deuterium concentration in the uncoated and coated samples with and without gamma-ray irradiation were investigated by nuclear reaction analysis (NRA), which is according to the nuclear reaction of $D(^3He, p)^4He$. NRA was carried out using a tandem accelerator at Max-Planck-Institut für Plasmaphysik (IPP), Garching. ^3He ion beam in the energy range of 0.69–4.5 MeV was used as the probe beam. In the depth profile analysis, chemical composition of the sample surface and the coating thickness were analyzed by Rutherford backscattering spectrometry (RBS). The thickness of Y_2O_3, SiC, and ZrO_2 coatings was estimated to be 2.2–3.5, 0.48–0.64 and 0.88 μm, respectively. After that, deuterium depth profiles in the samples were optimized from detected proton spectra with two analysis softwares: SIMNRA7.01 [11] and MultiSIMNRA1.4.0.915 [12].

Table 1 Summary of gamma-ray irradiation parameters

Dose / kGy	Dose rate / Gy s^{-1}	Facility
1	0.084–0.096	Shizuoka University
10	0.335–0.384	
100		
1280	2.43	QST

3. Results and discussion

3.1. Structural analysis

3.1.1. F82H substrate

It was worth investigating the F82H surface after deuterium exposure because the surface color turned white. Fig. 2 shows XPS spectra for the F82H substrate after deuterium exposure. From the results of the chemical shift of the spectra, chromium oxide (Cr_2O_3) formation was confirmed. It should be noted that this sample is an "uncoated" F82H steel but formed a Cr_2O_3 layer might show a different deuterium retention behavior from the original F82H surface to a depth of more than 100 nm.

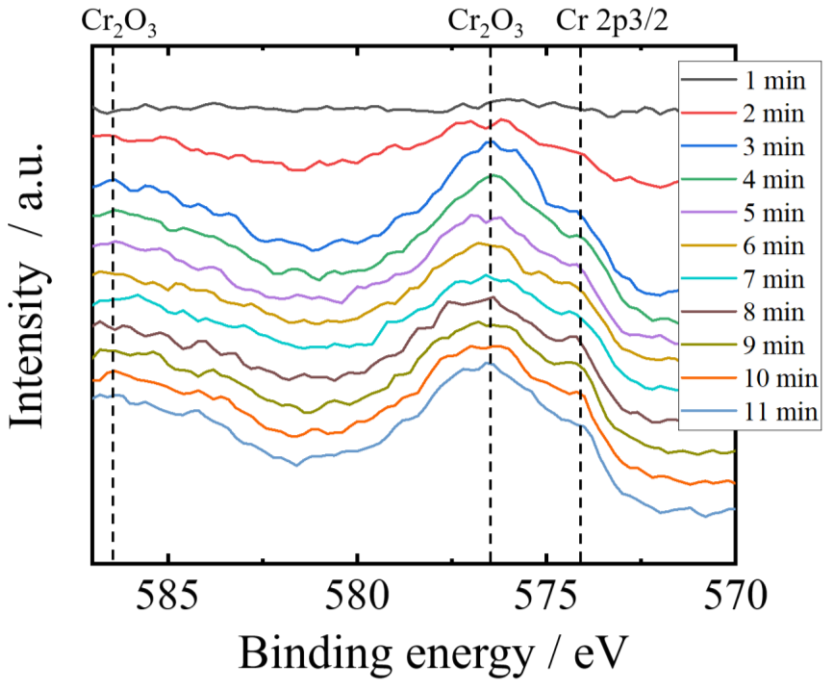

Fig. 2 XPS spectra of chromium in F82H substrate after deuterium exposure with Ar sputtering of up to 11 min. Sputtering rate was approximately 10 nm min^{-1}.

3.1.2. Ceramic coatings

GIXRD spectra of Y_2O_3, SiC and ZrO_2 coatings were shown in Fig. 3. From the spectrum of the Y_2O_3 coating, peaks of the cubic phase were confirmed at around 29 º, 45 º and 49 º. The peak at 29 º was the sharpest of all the peaks, and the grain size was estimated to be 17 nm. In contrast, only a peak of α-iron at 45 º deriving from F82H substrate was observed in the spectrum of the SiC coating. According to our previous study, the SiC coating fabricated by MS at room temperature showed no significant diffraction peaks, suggesting that the coating had an amorphous state or even no short-range order [3]. A strong diffraction peak deriving from the tetragonal phase was confirmed at around

147 31 º in the ZrO_2 coating fabricated by MOD. The grain size was calculated to be approximately 6 nm.
148 From these results, Y_2O_3 and ZrO_2 coatings had crystalline structures, and SiC coating consisted of a
149 non-crystalline structure.

150 Elemental depth profiles for the SiC and ZrO_2 coatings were shown in Figs. 4 and 5, respectively.
151 In the SiC coating, an atomic concentration of oxygen increased from 10 to 30 at% with depth.
152 Chemical state of the oxygen in the coating showed the existence of some kinds of compounds as
153 impurities. High atomic concentrations of carbon at both coating surfaces were considered as
154 contamination, while the carbon impurity of around 15 at% was also detected inside the ZrO_2 coating,
155 which was derived from the precursor.

156

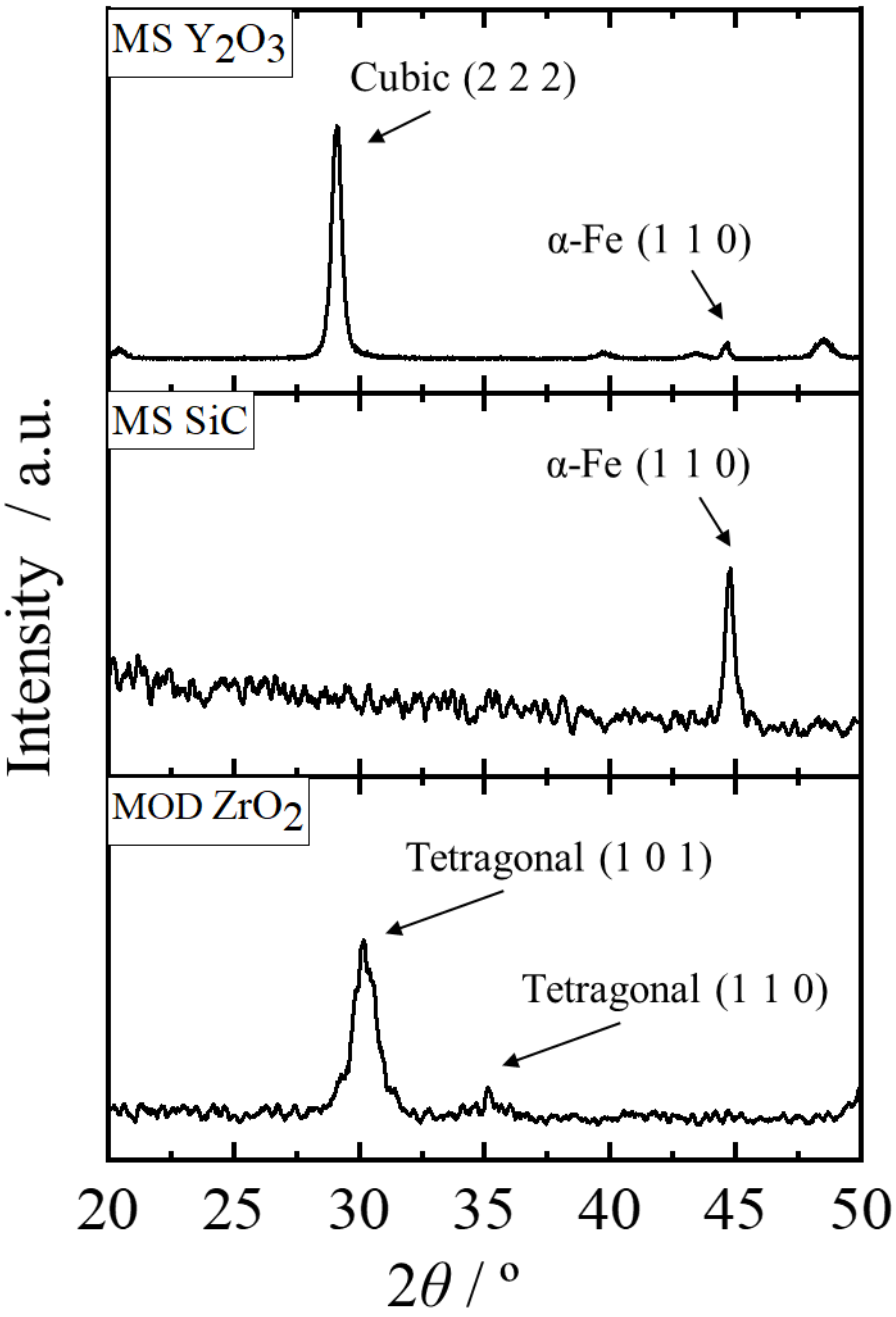

157

158 Fig. 3. GIXRD spectra of three kinds of ceramic coatings.

159

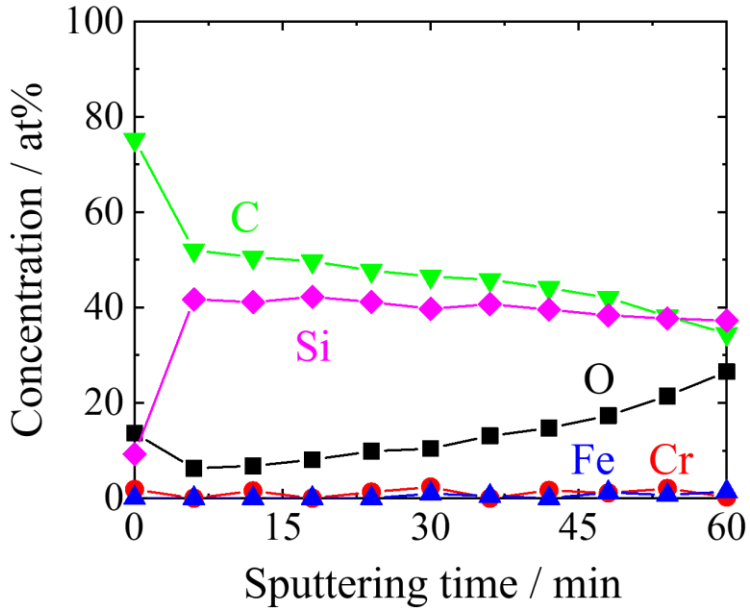

160

161 Fig. 4. XPS elemental depth profiles for SiC coating prepared by MS.

162

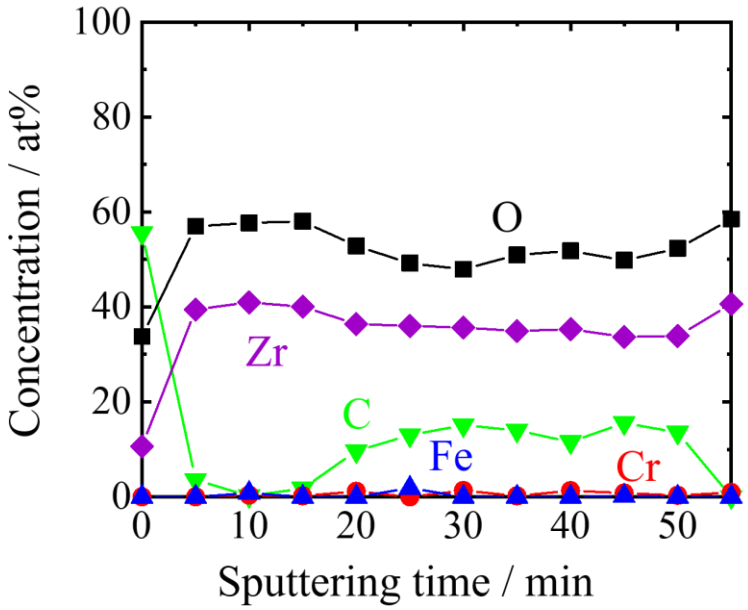

163

164 Fig. 5. XPS elemental depth profiles for ZrO_2 coating prepared by MOD.

165

3.2. Deuterium retention behavior

Deuterium depth profiles of the F82H substrate, Y_2O_3, SiC and ZrO_2 coatings with and without gamma-ray irradiation are shown in Figs. 6–9. Sample number denotes the conditions of deuterium exposure and irradiation. Samples #1 are blank samples without deuterium exposure and gamma-ray irradiation, and the other samples were exposed to 80-kPa deuterium for 50 h at 500 ºC. Samples #2 were not irradiated. Samples #3 were irradiated with the dose of 1 kGy (dose rate: < 0.096 Gy s^{-1}). Samples #4 and #5 were irradiated with the doses of 10 and 100 kGy (dose rate: 0.335–0.384 Gy s^{-1}), respectively. Irradiation with the highest dose of 1280 kGy and dose rate of 2.43 Gy s^{-1} was conducted for Samples #6.

In this section, deuterium retention behaviors of the F82H and coatings without irradiation are firstly mentioned. The deuterium concentration in the F82H samples was constant around 0.01 at% except for the surface region where the concentration was 0.05 at%. It is obvious that the deuterium retention in F82H was relatively small due to a high diffusivity. In contrast, the Cr_2O_3 layer formed during the deuterium exposure had a larger retention of deuterium.

Deuterium was distributed uniformly in the coating for the Y_2O_3-coated samples. Compared to Sample #2 of the F82H, the deuterium concentrations in the coatings were 1–3 orders of magnitude higher. In the previous studies of deuterium retention behavior on erbium oxide (Er_2O_3) coatings [6,13,14], it was considered that deuterium accumulated and/or diffuse along grain boundaries in the coatings. In this study, Y_2O_3 and ZrO_2 coatings were polycrystalline, and thus deuterium would also

185 remain in grain boundaries of these two ceramic coatings. If a ceramic coating had a homogeneous
186 grain density, the deuterium concentration should decrease with depth according to Fick's law on
187 atomic diffusion in solids. In the case of the Y_2O_3 coatings deposited by MS, the grain size near the
188 interface between the coating and the substrate became smaller than that at the outermost surface [2].
189 In other words, the density of deuterium-trapping sites increased with depth. That would be a reason
190 why the deuterium concentration in the coatings seemed constant.

191 In the SiC-coated samples, the deuterium concentration gradually increased toward the coating-
192 substrate interface and was remarkably higher (~10 at%) than that in the other uncoated and coated
193 samples. Deuterium probably remains in the coating as chemical states of Si-D and C-D [15].
194 Moreover, these results indicate that non-crystalline SiC coating has an extremely large number of
195 deuterium-trapping sites due to the fact that the coating has no grains where deuterium diffuses slower.
196 Another point is that the deuterium concentration increased toward the coating-substrate interface,
197 and the trend of the deuterium depth profiles corresponded to that of oxygen confirmed in the XPS
198 analysis (Fig. 4). Therefore, Si-O-C compounds might have a high deuterium retention capability.

199 Deuterium depth distribution of ZrO_2 coatings showed that the outermost surface contained the
200 highest concentration in the coating, and the deuterium concentration steeply decreased in subsurface.
201 From the result of XPS elemental depth profile shown in Fig. 5, the trend of the concentration of
202 carbon corresponded to that of the deuterium depth profiles, indicating carbon impurity might
203 increase deuterium retention.

From these results, it is suggested that deuterium retention strongly depended on coating materials, fabrication methods and crystal structures. Ceramic coatings tend to retain a larger amount of deuterium than F82H, and non-crystalline structure would make an extremely large contribution to deuterium retention in comparison with crystalline one. In addition, impurities might influence deuterium retention behaviors in the coatings.

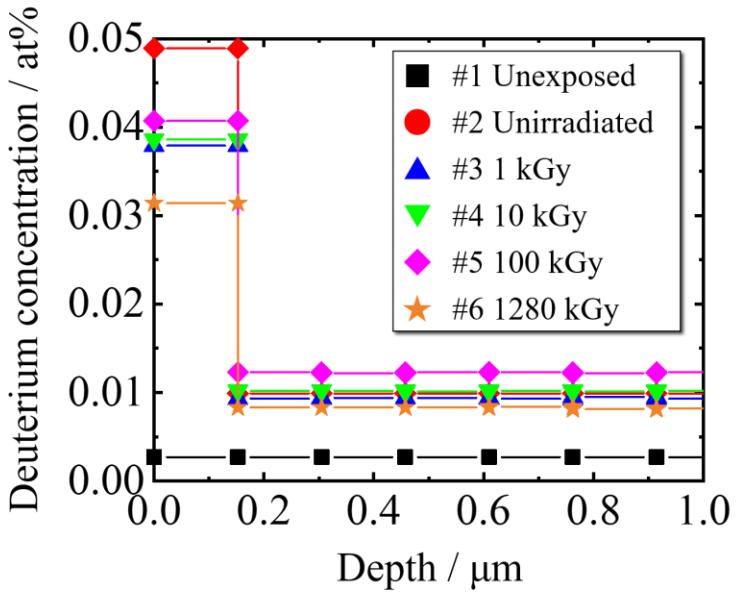

Fig. 6. Deuterium depth profiles of F82H samples with and without deuterium exposure and gamma-ray irradiation.

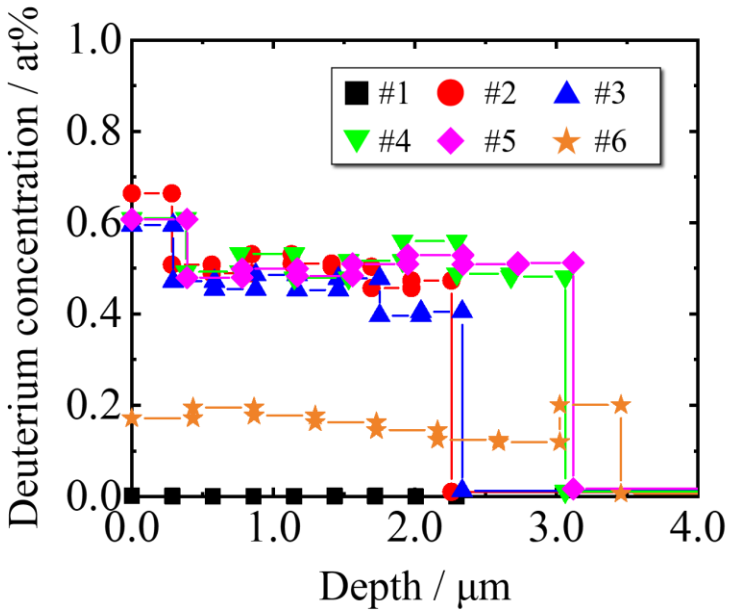

214

215 Fig. 7. Deuterium depth profiles of Y_2O_3 coatings with and without deuterium exposure and

216 gamma-ray irradiation.

217

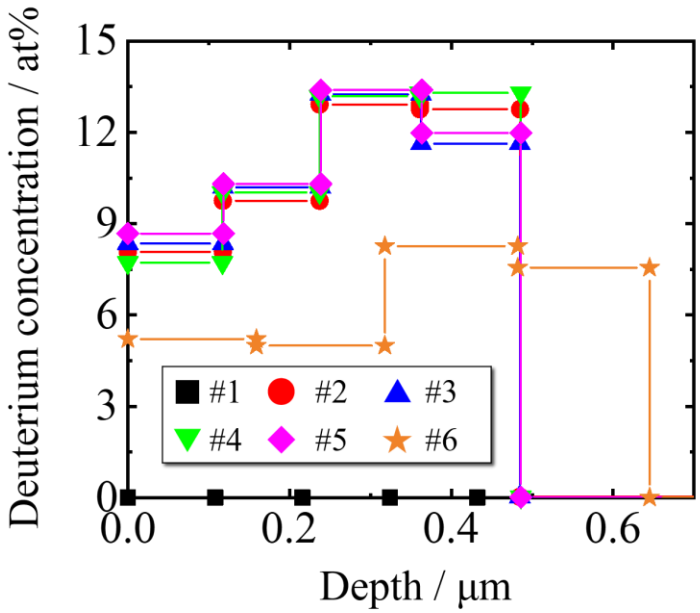

218

219 Fig. 8. Deuterium depth profiles of SiC coatings with and without deuterium exposure and gamma-

220 ray irradiation.

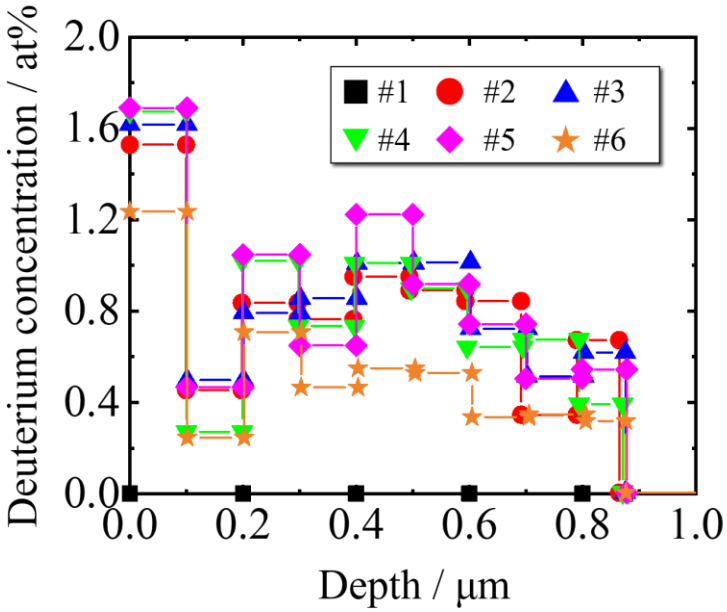

Fig. 9. Deuterium depth profiles of ZrO_2 coatings with and without deuterium exposure and gamma-ray irradiation.

3.3. Gamma-ray irradiation effect

Deuterium retention in the outermost surface of the F82H samples, where the Cr_2O_3 layer formed during deuterium exposure, exhibited a clear tendency to decrease with irradiation dose, as shown in Fig. 6. This result would be an explicit evidence that gamma-ray irradiation promoted deuterium desorption at the oxide surface. In the Y_2O_3-coated samples with the dose of up to 100 kGy and the dose rate of 0.084–0.384 Gy s^{-1}, the correlation between irradiation and deuterium retention was not clear. However, the retention drastically decreased in the sample with the dose of 1280 kGy and the one order of magnitude higher dose rate of 2.43 Gy s^{-1}. In this case, the deuterium retention might be

more dependent on the dose rate than the dose, because the deuterium retention in the samples irradiated with the dose of 10 and 100 kGy at the same dose rate did not change. In the case of the SiC and ZrO_2 coatings, as is the case with the Y_2O_3 coatings, deuterium concentration significantly decreased for the samples irradiated with the dose rate of 2.43 Gy s^{-1}. In the previous study, gamma-ray irradiation experiments were conducted for 80 days with the dose rate of 0.14–0.19 Gy s^{-1} for the investigation of gamma-ray irradiation influence on hydrogen isotope transport in Zircaloy-4 [16]. Although the reached absorbed dose was about 1 MGy, the deuterium diffusion in Zircaloy-4 was not confirmed. For further discussion, deuterium atomic concentrations per unit volume at each gamma-ray absorbed dose were calculated. For example, in the ZrO_2 coatings, the concentration of the samples irradiated up to 100 kGy with the dose rate of 0.084–0.384 Gy s^{-1} were approximately 7.9×10^{20} D cm^{-3}, and that of samples irradiated up to 1280 kGy with the dose rate of 2.43 Gy s^{-1} was approximately 5.0×10^{20} D cm^{-3}. The decrease of the deuterium concentration in all the examined materials at the dose rate of 2.43 Gy s^{-1} was confirmed. Hence, the gamma-ray irradiation effect on deuterium retention in the ceramic coatings would have a threshold dose rate which promotes deuterium diffusion and desorption.

The decrease of deuterium retention in ceramic coatings by gamma-ray irradiation can be explained by the following process. Compton scattering is a major interaction between the gamma rays from ^{60}Co (1.17 and 1.33 MeV) and the coating materials, which generates a gamma ray with a lower energy and an electron. Under the gamma-ray irradiation environment, deuterium atoms in the

ceramics are likely to be excited and have a higher potential energy for surface reactions and diffusion. Chemically, the activated deuterium could break a chemical bond with an atom in the ceramics such as oxygen and carbon, and diffuse in and desorb from the ceramics, resulting in the decrease of deuterium retention. In addition, it is considered that deuterium diffusion and desorption would not be promoted unless the number of Compton electrons per unit time and volume exceeds a certain value because the activated state of deuterium would not be maintained. From this reason, the gamma-ray irradiation effect on deuterium retention in the ceramic coatings would have a threshold dose rate. However, details of the gamma-ray irradiation effects on hydrogen isotope diffusion and desorption were not elucidated in this study. It is necessary to further investigate the effects to fusion reactor materials, in particular in a wider gamma-ray energy range and a higher dose rate to cover fusion reactor environments.

4. Summary

Gamma-ray irradiation effects on deuterium retention in F82H substrates and three kinds of ceramic coatings were investigated through deuterium exposure, gamma-ray irradiation using ^{60}Co sources and deuterium depth analysis. The deuterium retention behavior was clearly varied by coating materials, fabrication methods and microstructures. The amount of deuterium retention in ceramic coatings was larger than that in the F82H substrates, and that in the non-crystalline coating was much higher than the crystalline ones. Besides, carbon and oxygen impurities would increase deuterium retention in the coatings. The gamma-ray irradiation experiments showed that a change in deuterium

retention in the coatings was not clear at the dose rate of 0.084–0.384 Gy s^{-1}, while a significant decrease of the amount of deuterium retention was confirmed at the dose rate of 2.43 Gy s^{-1}. The gamma-ray irradiation effect would have a threshold dose rate to promote deuterium diffusion and/or desorption. The acceleration of deuterium diffusion and desorption in the materials under gamma-ray irradiation would be derived from excitation of deuterium by Compton electrons. The excited state of deuterium would be maintained by gamma-ray irradiation with more than the threshold dose rate. Further investigations are necessary to elucidate the irradiation effects with a wider gamma-ray energy range and higher dose rates for the simulation of fusion reactor environments.

Acknowledgments

This work was supported by JSPS KAKENHI Grant Number 15H05562, Fusion Engineering Division, Atomic Energy Society of Japan, and the general collaboration research with National Institute for Fusion Science (NIFS18KUHR051). A part of this work was conducted at Advanced Characterization Nanotechnology Platform of the University of Tokyo, supported by "Nanotechnology Platform" of the Ministry of Education, Culture, Sports, Science and Technology (MEXT), Japan.

References

[1] Ch. Linsmeier et al., Development of advanced high heat flux and plasma-facing materials, Nuclear Fusion 57 (2017) 092007 (60pp).

[2] T. Chikada et al., Deuterium permeation behavior and its iron-ion irradiation effect in yttrium oxide coating deposited by magnetron sputtering, Journal of Nuclear Materials 511 (2018) 560–566.

[3] T. Chikada et al., Deuterium permeation and thermal behaviors of amorphous silicon carbide coatings on steels, Fusion Engineering and Design 86 (2011) 2192–2195.

[4] T. Chikada et al., Fabrication technology development and characterization of tritium permeation barriers by a liquid phase method, Fusion Engineering and Design 136 (2018) 215–218.

[5] S. Horikoshi et al., Deuterium permeation and retention behaviors in erbium oxide-iron multilayer coatings, Fusion Engineering and Design 124 (2017) 1086–1090.

[6] R. Sato et al., Measurement of hydrogen isotope concentration in erbium oxide coating, Fusion Engineering and Design 89 (2014) 1375–1379.

[7] H. Fujita et al., Deuterium permeation through metals under γ-ray irradiation, Fusion Engineering and Design 133 (2018) 95–98.

[8] H. Fujita et al., The effects of γ-ray irradiation on deuterium permeation through reduced activation ferritic steel and erbium oxide coating, Nuclear Materials and Energy 17 (2018) 78–82.

[9] T. Tanaka et al., Control of substrate oxidation in MOD ceramic coating on low-activation ferritic steel with reduced-pressure atmosphere, Journal of Nuclear Materials 455 (2014) 630–634.

[10] M. Matsunaga et al., Lithium-lead corrosion behavior of erbium oxide, yttrium oxide and zirconium oxide coatings fabricated by metal organic decomposition, Journal of Nuclear Materials 511 (2018) 537–543.

[11] M. Mayer, SIMNRA User's Guide, Report IPP 9/113, Max-Planck-Institut für Plasmaphysik, Garching, Germany, 1997.

[12] T.F. Silva et al., MultiSIMNRA: A computational tool for self-consistent ion beam analysis using SIMNRA, Nuclear instruments and Methods in Physics Research Section B: Beam Interactions with Materials and Atoms 371 (2016) 86.

[13] T. Chikada et al., Microstructure change and deuterium permeation behavior of erbium oxide coating, Journal of Nuclear Materials 417 (2011) 1241–1244.

[14] W. Mao et al., Hydrogen diffusion along grain boundaries in erbium oxide coatings, Journal of Nuclear Materials 455 (2014) 360–365.

[15] M. T. Koller et al., Deuterium retention in silicon carbide, SiC ceramic matrix composites, and SiC coated graphite, Nuclear Materials and Energy 20 (2019) 100704.

[16] F. A. Martin et al., Influence of γ-irradiation on the transport kinetics of hydrogen in pre-transition oxidized Zircaloy-4 at room temperature, Journal of Nuclear Materials 465 (2015) 615–625.